*Int. J. Solids Structures* Vol. 19, No. 8, pp. 693–707, 1983
Printed in Great Britain.

0020-7683/83 $3.00 + .00


# THE EFFECTIVE MODULI OF SHORT-FIBER COMPOSITES

JACOB ABOUDI
Department of Solid Mechanics, Materials and Structures, Faculty of Engineering, Tel-Aviv University, Ramat-Aviv 69978, Israel

(*Received* 9 *August* 1982; *in revised form* 6 *December* 1982)

**Abstract**—A first order continuum theory with microstructure is developed for aligned short-fiber composites. The fibrous material is modeled by a triply periodic array of rectangular parallelpiped elastic fibres which are embedded in an elastic matrix. A proper reduction of the theory, by which the microstructure variables are eliminated, yields the effective moduli of the short-fiber composite. The overall elastic constants of the three specific situations of long-fiber composites, particulate composites and periodically bilaminated media, are obtained as special cases. The reliability of the predicted effective moduli is verified by numerous comparisons with available experimental results in various cases.

## INTRODUCTION

The prediction of the elastic effective moduli of fiber-reinforced composite materials, in the case when the fibers are continuous, is well established, see Christensen[1] and references cited there. When short-fiber composites are considered, the problem of the determination of the overall behavior becomes more complicated, due to the additional effect of the finiteness of the fibers, as a result of which the moduli depend this time, in particular, on the fibers' aspect ratio (ratio of length to width).

Under dilute conditions, when the concentration of the fibers in the matrix is low enough, it is possible to neglect the interaction effects between the fibers. Consequently, one can deal with a single inclusion (ellipsoid) imbedded in the matrix, and Russel[2] derived the effective moduli under the additional assumption of a slender inclusion. Similarly, Phan-Thien[3] applied recently the slender-body approximation to a dilute suspension of fibers, in order to obtain the effective moduli of short-fiber composites with arbitrary distribution of fibers.

The self-consistent method has been applied recently in [4] and [5] for the prediction of the effective constants of short-fiber composites. In the framework of this theory, the elastic field of the dense fibers is approximated by the field of an isolated ellipsoidal inclusion. The single inclusion is assumed to be imbedded in a continuous homogeneous medium. The inclusion has the elastic properties of the short fiber, while the surrounding material possesses the effective properties of the composite. The solution of the single elastic inclusion problem is used for the determination of the overall constants of the composites. Thus, the method employs the same elastic solution as in the dilute case. These assumptions give rise to some unrealistic descriptions of the composite material by the self-consistent method, as it is discussed in [1].

A high order continuum theory with microstructure for unidirectional long-fiber viscoplastic composites was developed by Aboudi[6]. The continuous fibers have square cross sections and are embedded in the matrix in the form of a square array. An appropriate reduction of the theory by which the microstructure variables are eliminated, yields the effective behavior of the composite. For elastic composites it turns out that the values of the four effective constants for the axial Young's modulus and Poisson's ratio, the plane strain bulk modulus and the axial shear modulus given by this theory, are in excellent agreement with the values computed from the exact expressions of the corresponding moduli predicted by the composite cylinders model[7, 1]. Whereas it is not possible to derive from the composite cylinders model an exact expression for the effective transverse Young's modulus and only bounds are available, the continuum theory of[6] determines directly this constant as well. The veracity of this constant is checked by comparisons with experimental results exhibiting good agreement.

In this paper, the approach of Ref. [6] is generalized to model short-fiber composites. However, since the overall behavior of the composite is sort, the development is confined here to a first order theory, which is reduced by the elimination of the microstructure variables to

yield the required effective constants. The short fibers are modeled by rectangular parallelepipeds, which are imbedded in the matrix in the form of a triply periodic array. The effective Young's moduli and Poisson's ratios of the composite are determined from the solution of a system of algebraic equations.

In the special case of long square parallelpipeds, the effective constants of long-fiber composites of [6] are recovered. Furthermore, in the limiting situation, when two sides of the rectangular parallelpiped are very long with respect to the third one, the case of a periodically bilaminated medium is obtained. It is well known that the overall behavior of a bilaminated composite can be represented by a transversely isotropic material whose five effective constants are given by exact expressions (see Postma[8]). It turns out that the effective constants provided by the present theory apparently coincide with those computed from the exact expressions of Postma.

When the aspect ratio of the fibers is equal to one, the special case of a particulate composite is obtained, in which the particles are represented by cubic inclusions and the effective constants can be readily computed. If, on the other hand, the particulate medium is modeled by the composite spheres model[9, 1], it is known that only the effective bulk modulus can be obtained in an exact form. Here it turns out that the values of the bulk modulus predicted by the present model are in excellent agreement with those given by the closed form expression of the composite spheres model.

The reliability of the effective moduli given by the proposed model is checked by several comparisons with available experimental data for particulate and short-fiber composites, which indicate satisfactory agreements. Comparisons with the results based on the self-consistent method are given and discussed.

## GEOMETRY AND DISPLACEMENT EXPANSION

Consider a compsoite material which consists of an elastic matrix reinforced by unidirectional elastic fibers of finite length. It is assumed that the fibers have the form of a rectangular parallelpiped whose volume is $d_1h_1l_1$ and are imbedded in the matrix in a triply periodic array in the $x_1$, $x_2$ and $x_3$ directions (see Fig. 1a). Let $d_2$, $h_2$ and $l_2$ represent the spacing of the fibers within the matrix in the $x_1$, $x_2$ and $x_3$ directions, respectively.

Due to the assumed regular array, we consider a representative cell of dimensions $(d_1+d_2)$, $(h_1+h_2)$, $(l_1+l_2)$, as shown in Fig. 1(b). The cell is divided into eight subcells $\alpha, \beta, \gamma = 1, 2$ and eight local systems of coordinates $(\bar{x}_1^{(\alpha)}, \bar{x}_2^{(\beta)}, \bar{x}_3^{(\gamma)})$ are introduced whose origins are located at the center of each subcell. Their positions are denoted by $x_1^{(\alpha)}, x_2^{(\beta)}, x_3^{(\gamma)}$.†

A high order continuum theory can be developed for the modeling of the composite, which is based on the expansion of the displacement vector in each subcell, in terms of the distances in the $x_1$, $x_2$ and $x_3$ directions from its center. This expansion can be expressed in terms of the Legendre polynomials permitting the modeling of increasing complex deformation patterns within the subcell. This paper is confined to the development of a first order theory which is sufficient for the extraction of the average behavior of the composite by a proper reduction.

For a first order theory, the displacement components at any point within the subcell can be expressed as

$$u_i^{(\alpha\beta\gamma)} = w_i^{(\alpha\beta\gamma)} + \bar{x}_1^{(\alpha)}\phi_i^{(\alpha\beta\gamma)} + \bar{x}_2^{(\beta)}\chi_i^{(\alpha\beta\gamma)} + \bar{x}_3^{(\gamma)}\psi_i^{(\alpha\beta\gamma)} \quad i = 1, 2, 3 \tag{1}$$

where $w_i^{(\alpha\beta\gamma)}(x_1^{(\alpha)}, x_2^{(\beta)}, x_3^{(\gamma)}, t)$ are the displacement components at the center point of the subcell, and $\phi_i^{(\alpha\beta\gamma)}(x_1^{(\alpha)}, x_2^{(\beta)}, x_3^{(\gamma)}, t)$, $\chi_i^{(\alpha\beta\gamma)}(x_1^{(\alpha)}, x_2^{(\beta)}, x_3^{(\gamma)}, t)$ and $\psi_i^{(\alpha\beta\gamma)}(x_1^{(\alpha)}, x_2^{(\beta)}, x_3^{(\gamma)}, t)$ characterize the linear dependence of the displacements on the local coordinates within the subcell, and $t$ is the time.

According to (1) the displacement field in the composite is given in terms of $w_i^{(\alpha\beta\gamma)}$, $\phi_i^{(\alpha\beta\gamma)}$, $\chi_i^{(\alpha\beta\gamma)}$ and $\psi_i^{(\alpha\beta\gamma)}$ and these are defined only at the discrete points $x_1 = x_1^{(\alpha)}$, $x_2 = x_2^{(\beta)}$, $x_3 = x_3^{(\gamma)}$. By a smoothing operation the discrete nature of the composite can be eliminated and a

†Here and in the sequel the subscripts or superscripts $\alpha$, $\beta$, $\gamma$ will indicate that quantities belong to one of the subcells. Repeated $\alpha$ or $\beta$ or $\gamma$ do not imply summation.

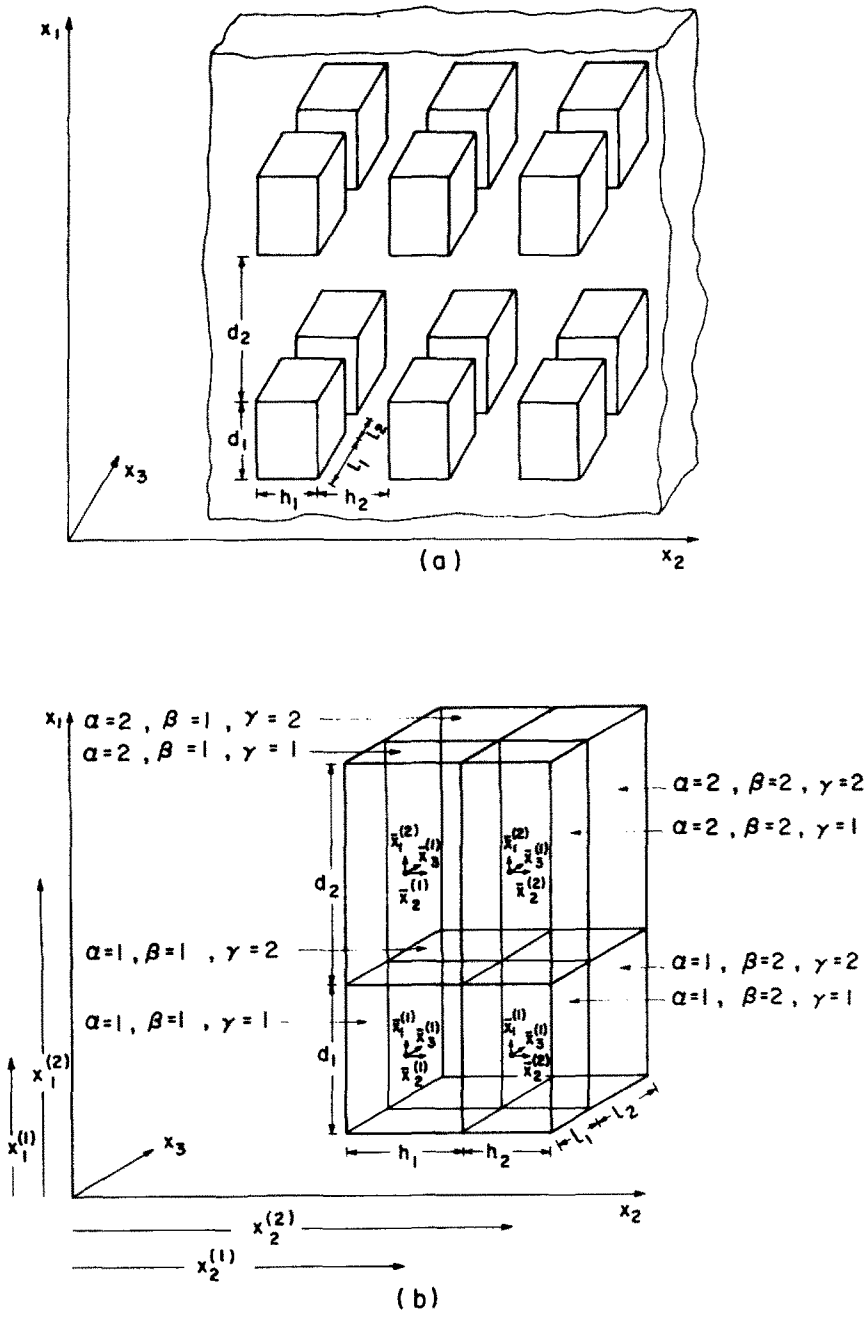


Fig. 1. (a) A short-fiber composite in which the rectangular parallelpiped fibers are arranged in a triply periodic array. (b) A representative cell.

homogeneous continuum model is obtained. This is achieved by considering $w_i^{(\alpha\beta\gamma)}$, $\phi_i^{(\alpha\beta\gamma)}$, $\chi_i^{(\alpha\beta\gamma)}$ and $\psi_i^{(\alpha\beta\gamma)}$ as continuous functions of $x_1, x_2, x_3$ whose values at $x_1 = x_1^{(\alpha)}, x_2 = x_2^{(\beta)}, x_3 = x_3^{(\gamma)}$ coincide with the actual values at the centers of the subcells. This transition is indicated by writing $(x_1, x_2, x_3, t)$ instead of $(x_1^{(\alpha)}, x_2^{(\beta)}, x_3^{(\gamma)}, t)$ for the arguments of the field variables. Consequently, both types of materials are assumed to exist simultaneously at every point of the continuum model.

The components of the small strain tensor are given by

$$\epsilon_{ij}^{(\alpha\beta\gamma)} = \tfrac{1}{2}[\partial_i u_j^{(\alpha\beta\gamma)} + \partial_j u_i^{(\alpha\beta\gamma)}] \quad i, j = 1, 2, 3 \tag{2}$$

where the differentiations are with respect to the local coordinates, i.e. $\partial_1 = \partial/\partial \bar{x}_1^{(\alpha)}$, $\partial_2 = \partial/\partial \bar{x}_2^{(\beta)}$ and $\partial_3 = \partial/\partial \bar{x}_3^{(\gamma)}$.

## INTERFACE CONTINUITY CONDITIONS

Along the interfaces of the subcells the displacements and normal and shear stresses are continuous, i.e.

$$u_i^{(1\beta\gamma)}\Big|_{\bar{x}_1^{(1)}=\pm d_1/2} = u_i^{(2\beta\gamma)}\Big|_{\bar{x}_1^{(2)}=\mp d_2/2} \tag{3}$$

$$u_i^{(\alpha 1\gamma)}\Big|_{\bar{x}_2^{(1)}=\pm h_1/2} = u_i^{(\alpha 2\gamma)}\Big|_{\bar{x}_2^{(2)}=\mp h_2/2} \tag{4}$$

$$u_i^{(\alpha\beta 1)}\Big|_{\bar{x}_3^{(1)}=\pm l_1/2} = u_i^{(\alpha\beta 2)}\Big|_{\bar{x}_3^{(2)}=\mp l_2/2} \tag{5}$$

$$\sigma_{1i}^{(1\beta\gamma)}\Big|_{\bar{x}_1^{(1)}=\pm d_1/2} = \sigma_{1i}^{(2\beta\gamma)}\Big|_{\bar{x}_1^{(2)}=\mp d_2/2} \tag{6}$$

$$\sigma_{2i}^{(\alpha 1\gamma)}\Big|_{\bar{x}_2^{(1)}=\pm h_1/2} = \sigma_{2i}^{(\alpha 2\gamma)}\Big|_{\bar{x}_2^{(2)}=\mp h_2/2} \tag{7}$$

$$\sigma_{3i}^{(\alpha\beta 1)}\Big|_{\bar{x}_3^{(1)}=\pm l_1/2} = \sigma_{3i}^{(\alpha\beta 2)}\Big|_{\bar{x}_3^{(2)}=\mp l_2/2} \tag{8}$$

where $\sigma_{ij}^{(\alpha\beta\gamma)}(i, j = 1, 2, 3)$ are the stress components within the subcell, and the plus-and-minus signs in eqns (3) and (6) denote the two different equations obtained, depending on whether the interface follows the subcell $(1\beta\gamma)$ or $(2\beta\gamma)$. Similarly, the plus-and-minus signs in eqns (4), (7) and (5), (8) denote the two different situations depending on whether the corresponding interface follows the subcell $(\alpha 1\gamma)$ or $(\alpha 2\gamma)$ and $(\alpha\beta 1)$ or $(\alpha\beta 2)$, respectively.

Generalizing the procedure given in [6] for infinitely long fibers, it can be shown that the displacement continuity conditions (3)–(5) yield in the present case, when the fibers have a finite length, the following relations (in the framework of the first order theory), compare Ref. [6, eqns (54)]:

$$\begin{aligned} w_i^{(111)} = w_i^{(112)} = w_i^{(121)} = w_i^{(122)} = w_i^{(211)} = w_i^{(212)} \\ = w_i^{(221)} = w_i^{(222)} \equiv w_i(x_1, x_2, x_3, t), \end{aligned} \tag{9}$$

$$\begin{aligned} d_1\phi_i^{(1\beta\gamma)} + d_2\phi_i^{(2\beta\gamma)} &= (d_1 + d_2)\frac{\partial}{\partial x_1} w_i \\ h_1\chi_i^{(\alpha 1\gamma)} + h_2\chi_i^{(\alpha 2\gamma)} &= (h_1 + h_2)\frac{\partial}{\partial x_2} w_i \\ l_1\psi_i^{(\alpha\beta 1)} + l_2\psi_i^{(\alpha\beta 2)} &= (l_1 + l_2)\frac{\partial}{\partial x_3} w_i. \end{aligned} \tag{10}$$

Since the discrete nature of the medium is eliminated by the smoothing procedure, it is assumed that relations (10) hold simultaneously throughout the medium.

The transition from the discrete to the homogeneous continuum model replaces the stress continuity conditions (6)–(8) by

$$\begin{aligned} \sigma_{1i}^{(1\beta\gamma)}\left(x_k, \bar{x}_1^{(1)} = \pm\frac{d_1}{2}, \bar{x}_2^{(\beta)}, \bar{x}_3^{(\gamma)}, t\right) &= \sigma_{1i}^{(2\beta\gamma)}\left(x_k, \bar{x}_1^{(2)} = \mp\frac{d_2}{2}, \bar{x}_2^{(\beta)}, \bar{x}_3^{(\gamma)}, t\right) \\ \sigma_{2i}^{(\alpha 1\gamma)}\left(x_k, \bar{x}_1^{(\alpha)}, \bar{x}_2^{(1)} = \pm\frac{h_1}{2}, \bar{x}_3^{(\gamma)}, t\right) &= \sigma_{2i}^{(\alpha 2\gamma)}\left(x_k, \bar{x}_1^{(\alpha)}, \bar{x}_2^{(2)} = \mp\frac{h_2}{2}, \bar{x}_3^{(\gamma)}, t\right) \\ \sigma_{3i}^{(\alpha\beta 1)}\left(x_k, \bar{x}_1^{(\alpha)}, \bar{x}_2^{(\beta)}, \bar{x}_3^{(1)} = \pm\frac{l_1}{2}, t\right) &= \sigma_{3i}^{(\alpha\beta 2)}\left(x_k, \bar{x}_1^{(\alpha)}, \bar{x}_2^{(\beta)}, \bar{x}_3^{(2)} = \mp\frac{l_2}{2}, t\right) \end{aligned} \tag{11}$$

where $x_k$ stands for $x_1, x_2, x_3$. Equations (10) and (11) are 72 equations for the continuity of displacements and stresses, respectively.

## EQUATIONS OF MOTION

The equations of motion of the homogeneous continuum model are derived from the dynamic equations of motion in the subcell regions. In the absence of body forces, the latter are given by

$$\partial_i \sigma_{ij}^{(\alpha\beta\gamma)} = \rho_{\alpha\beta\gamma} \ddot{u}_j^{(\alpha\beta\gamma)},$$
$$|\bar{x}_1^{(\alpha)}| \le d_\alpha/2, |\bar{x}_2^{(\beta)}| \le h_\beta/2, |\bar{x}_3^{(\gamma)}| \le l_\gamma/2, i, j = 1, 2, 3 \tag{12}$$

where $\rho_{\alpha\beta\gamma}$ is the mass density of the material in the subcell, dots represent differentiation with respect to time, and the spatial differentiations are with respect to the local coordinates which are located at the centers of the subcells.

The equations of motion for the first order continuum theory are obtained by multiplying (12) by $(\bar{x}_1^{(\alpha)})^p (\bar{x}_2^{(\beta)})^q (\bar{x}_3^{(\gamma)})^r$; $p, q, r = 0, 1$; and integrating both sides with respect to $\bar{x}_1^{(\alpha)}$, $\bar{x}_2^{(\beta)}$ and $\bar{x}_3^{(\gamma)}$. This yields after integrations by parts and using (1) the following set of equations governing $w_j(x_k, t)$, $\phi_j^{(\alpha\beta\gamma)}(x_k, t)$, $\chi_j^{(\alpha\beta\gamma)}(x_k, t)$ and $\psi_j^{(\alpha\beta\gamma)}(x_k, t)$:

$$I_{1j(0,0,0)}^{(\alpha\beta\gamma)} + J_{2j(0,0,0)}^{(\alpha\beta\gamma)} + K_{3j(0,0,0)}^{(\alpha\beta\gamma)} = \rho_{\alpha\beta\gamma} \ddot{w}_j, \tag{13}$$

$$I_{1j(p,q,r)}^{(\alpha\beta\gamma)} + J_{2j(p,q,r)}^{(\alpha\beta\gamma)} + K_{3j(p,q,r)}^{(\alpha\beta\gamma)} - pS_{1j}^{(\alpha\beta\gamma)} - qS_{2j}^{(\alpha\beta\gamma)} - rS_{3j}^{(\alpha\beta\gamma)} = \tfrac{1}{12}\rho_{\alpha\beta\gamma}[\delta_{p1} d_\alpha^2 \ddot{\phi}_j + \delta_{q1} h_\beta^2 \ddot{\chi}_j + \delta_{r1} l_\gamma^2 \ddot{\psi}_j] \tag{14}$$

where $\delta_{ij}$ is the Kronecker delta, $q = r = 0$ when $p = 1$, $p = r = 0$ when $q = 1$, and $p = q = 0$ when $r = 1$. In (14)

$$I_{1j(p,q,r)}^{(\alpha\beta\gamma)} = \frac{1}{V_{\alpha\beta\gamma}} \left(\frac{d_\alpha}{2}\right)^p \int_{-h_\beta/2}^{h_\beta/2} \int_{-l_\gamma/2}^{l_\gamma/2} (\bar{x}_2^{(\beta)})^q (\bar{x}_3^{(\gamma)})^r \cdot$$
$$[\sigma_{1j}^{(\alpha\beta\gamma)}(d_\alpha/2) + (-1)^{p+1} \sigma_{1j}^{(\alpha\beta\gamma)}(-d_\alpha/2)]\, d\bar{x}_2^{(\beta)}\, d\bar{x}_3^{(\gamma)}, \tag{15}$$

$$J_{2j(p,q,r)}^{(\alpha\beta\gamma)} = \frac{1}{V_{\alpha\beta\gamma}} \left(\frac{h_\beta}{2}\right)^q \int_{-d_\alpha/2}^{d_\alpha/2} \int_{-l_\gamma/2}^{l_\gamma/2} (\bar{x}_1^{(\alpha)})^p (\bar{x}_3^{(\gamma)})^r \cdot$$
$$[\sigma_{2j}^{(\alpha\beta\gamma)}(h_\beta/2) + (-1)^{q+1} \sigma_{2j}^{(\alpha\beta\gamma)}(-h_\beta/2)]\, d\bar{x}_1^{(\alpha)}\, d\bar{x}_3^{(\gamma)}, \tag{16}$$

$$K_{3j(p,q,r)}^{(\alpha\beta\gamma)} = \frac{1}{V_{\alpha\beta\gamma}} \left(\frac{l_\gamma}{2}\right)^r \int_{-d_\alpha/2}^{d_\alpha/2} \int_{-h_\beta/2}^{h_\beta/2} (\bar{x}_1^{(\alpha)})^p (\bar{x}_2^{(\beta)})^q \cdot$$
$$[\sigma_{3j}^{(\alpha\beta\gamma)}(l_\gamma/2) + (-1)^{r+1} \sigma_{3j}^{(\alpha\beta\gamma)}(-l_\gamma/2)]\, d\bar{x}_1^{(\alpha)}\, d\bar{x}_2^{(\beta)}, \tag{17}$$

with

$$V_{\alpha\beta\gamma} = d_\alpha h_\beta l_\gamma \tag{18}$$

and

$$S_{ij}^{(\alpha\beta\gamma)} = \frac{1}{V_{\alpha\beta\gamma}} \int_{-d_\alpha/2}^{d_\alpha/2} \int_{-h_\beta/2}^{h_\beta/2} \int_{-l_\gamma/2}^{l_\gamma/2} \sigma_{ij}^{(\alpha\beta\gamma)}\, d\bar{x}_1^{(\alpha)}\, d\bar{x}_2^{(\beta)}\, d\bar{x}_3^{(\gamma)} \tag{19}$$

which is the average of the stress component in the subcell. In (15)–(17) $\sigma_{1j}^{(\alpha\beta\gamma)}(\pm d_\alpha/2)$, $\sigma_{2j}^{(\alpha\beta\gamma)}(\pm h_\beta/2)$ and $\sigma_{3j}^{(\alpha\beta\gamma)}(\pm l_\gamma/2)$ stand for the interfacial stresses $\sigma_{1j}^{(\alpha\beta\gamma)}(x_k, \bar{x}_1^{(\alpha)} = \pm d_\alpha/2, \bar{x}_2^{(\beta)}, \bar{x}_3^{(\gamma)}, t)$, $\sigma_{2j}^{(\alpha\beta\gamma)}(x_k, \bar{x}_1^{(\alpha)}, \bar{x}_2^{(\beta)} = \pm h_\beta/2, \bar{x}_3^{(\gamma)}, t)$ and $\sigma_{3j}^{(\alpha\beta\gamma)}(x_k, \bar{x}_1^{(\alpha)}, \bar{x}_2^{(\beta)}, \bar{x}_3^{(\gamma)} = \pm l_\gamma/2, t)$, respectively.

It can be seen from the stress continuity conditions (11) that the following relations are established

$$I_{1j(p,q,r)}^{(1\beta\gamma)} = (-1)^{p+1} I_{1j(p,q,r)}^{(2\beta\gamma)},$$
$$J_{2j(p,q,r)}^{(\alpha 1\gamma)} = (-1)^{q+1} J_{2j(p,q,r)}^{(\alpha 2\gamma)},$$
$$K_{3j(p,q,r)}^{(\alpha\beta 1)} = (-1)^{r+1} K_{3j(p,q,r)}^{(\alpha\beta 2)}. \tag{20}$$

## THE EFFECTIVE MODULI OF THE COMPOSITE

The overall behavior of the composite is determined by neglecting terms of the order of $d_\alpha^2$, $h_\beta^2$, $l_\gamma^2$ in (14) and eliminating the higher order displacement $\phi_j^{(\alpha\beta\gamma)}$, $\chi_j^{(\alpha\beta\gamma)}$ and $\psi_j^{(\alpha\beta\gamma)}$. The solution of the resulting equations, in conjunction with the continuity conditions (10) and (20), gives the effective moduli of the short-fiber composite when it is subjected to an appropriate type of loading. It should be noted that the omission of the second order terms enables the elimination of these microstructure variables, thus yielding relations between average quantities only (as shown in the sequel).

In performing this derivation it is assumed that the matrix and fibers are linearly isotropic elastic materials so that the stress–strain relations are given by the Hooke's law:

$$\sigma_{ij}^{(\alpha\beta\gamma)} = \lambda_{\alpha\beta\gamma}\epsilon_{kk}^{(\alpha\beta\gamma)}\delta_{ij} + 2\mu_{\alpha\beta\gamma}\epsilon_{ij}^{(\alpha\beta\gamma)} \qquad i, j, k = 1, 2, 3 \tag{21}$$

where $\lambda_{\alpha\beta\gamma}$ and $\mu_{\alpha\beta\gamma}$ are the Lamé constants of the material in the subcell $(\alpha\beta\gamma)$. Substituting (2) in (21), the average stress are readily obtained from (19) in the form

$$\begin{aligned}
S_{11}^{(\alpha\beta\gamma)} &= E_{\alpha\beta\gamma}\phi_1^{(\alpha\beta\gamma)} + \lambda_{\alpha\beta\gamma}[\chi_2^{(\alpha\beta\gamma)} + \psi_3^{(\alpha\beta\gamma)}],\\
S_{22}^{(\alpha\beta\gamma)} &= E_{\alpha\beta\gamma}\chi_2^{(\alpha\beta\gamma)} + \lambda_{\alpha\beta\gamma}[\phi_1^{(\alpha\beta\gamma)} + \psi_3^{(\alpha\beta\gamma)}],\\
S_{33}^{(\alpha\beta\gamma)} &= E_{\alpha\beta\gamma}\psi_3^{(\alpha\beta\gamma)} + \lambda_{\alpha\beta\gamma}[\phi_1^{(\alpha\beta\gamma)} + \chi_2^{(\alpha\beta\gamma)}],\\
S_{12}^{(\alpha\beta\gamma)} &= \mu_{\alpha\beta\gamma}[\chi_1^{(\alpha\beta\gamma)} + \phi_2^{(\alpha\beta\gamma)}],\\
S_{13}^{(\alpha\beta\gamma)} &= \mu_{\alpha\beta\gamma}[\psi_1^{(\alpha\beta\gamma)} + \phi_3^{(\alpha\beta\gamma)}],\\
S_{23}^{(\alpha\beta\gamma)} &= \mu_{\alpha\beta\gamma}[\psi_2^{(\alpha\beta\gamma)} + \chi_3^{(\alpha\beta\gamma)}],
\end{aligned} \tag{22}$$

with $E_{\alpha\beta\gamma} = \lambda_{\alpha\beta\gamma} + 2\mu_{\alpha\beta\gamma}$.

Neglecting second order terms in $d_\alpha^2$, $h_\beta^2$ and $l_\gamma^2$ in (14) yields

$$\begin{aligned}
I_{1j(1,0,0)}^{(\alpha\beta\gamma)} &= S_{1j}^{(\alpha\beta\gamma)},\\
J_{2j(0,1,0)}^{(\alpha\beta\gamma)} &= S_{2j}^{(\alpha\beta\gamma)},\\
K_{3j(0,0,1)}^{(\alpha\beta\gamma)} &= S_{3j}^{(\alpha\beta\gamma)}, \quad j = 1, 2, 3.
\end{aligned} \tag{23}$$

Equations (10), (20) and (23), in conjunction with the loading conditions, suffice for the determination of the effective axial ($x_1$-directions) Young's modulus and Poisson's ratio, and the effective transverse ($x_2$ and $x_3$-directions) Young's moduli and Poisson's ratios. This is illustrated in the sequel for oriented fibers (in the $x_1$-direction) of square cross section ($h_1 = l_1$) imbedded regularly in the matrix such that $h_2 = l_2$. In addition, the spacing of the fibers in the axial direction $x_1$ is taken to be equal to the spacing in the transverse directions, i.e. $d_2 = h_2 = l_2$. Let $s$ denote the fiber aspect ratio: $s = d_1/h_1$. Accordingly, the volume fraction of the fibers is given by

$$v_1 = \frac{sh_1^3}{(h_1 + h_2)^2(sh_1 + h_2)} \tag{24}$$

from which $h_1/h_2$ can be determined for given values of $v_1$ and $s$.

The average stresses in the composite are given by

$$\sigma_{ij} = \frac{1}{V}\sum_{\alpha,\beta,\gamma=1}^{2} V_{\alpha\beta\gamma}S_{ij}^{(\alpha\beta\gamma)} \tag{25}$$

where $V = (d_1 + d_2)(h_1 + h_2)(l_1 + l_2)$ being the total volume of the representative cell. Similarly, the average strain has the form

$$\bar{\sigma}_{ij} = \frac{1}{V}\sum_{\alpha,\beta,\gamma=1}^{2} V_{\alpha\beta\gamma}\epsilon_{ij}^{(\alpha\beta\gamma)} \tag{26}$$

which is also compatible with the expression

$$\bar{\epsilon}_{ij} = \frac{1}{2}\left(\frac{\partial}{\partial x_i} w_j + \frac{\partial}{\partial x_j} w_i\right) \tag{27}$$

as can be verified from (1), (2) and (10).

Suppose that the composite is subjected to a uniaxial stress in the $x_1$-direction, such that $\bar{\sigma}_{11} \neq 0$, and all other $\bar{\sigma}_{ij}$ are zero. In this situation the following 26 nontrivial algebraic equations in the 26 unknowns $\phi_1^{(\alpha\beta\gamma)}$, $\chi_2^{(\alpha\beta\gamma)}$, $\psi_3^{(\alpha\beta\gamma)}$, $(\partial/\partial x_2)w_2$ and $(\partial/\partial x_3)w_3$ are obtained from (20), (23) and (10):

$$\begin{gathered}
S_{11}^{(1\beta\gamma)} = S_{11}^{(2\beta\gamma)}, \\
S_{22}^{(\alpha 1\gamma)} = S_{22}^{(\alpha 2\gamma)}, \\
S_{33}^{(\alpha\beta 1)} = S_{33}^{(\alpha\beta 2)}, \\
d_1\phi_1^{(1\beta\gamma)} + d_2\phi_1^{(2\beta\gamma)} = (d_1 + d_2)\frac{\partial}{\partial x_1} w_1, \\
h_1\chi_2^{(\alpha 1\gamma)} + h_2\chi_2^{(\alpha 2\gamma)} = (h_1 + h_2)\frac{\partial}{\partial x_2} w_2, \\
l_1\psi_3^{(\alpha\beta 1)} + l_2\psi_3^{(\alpha\beta 2)} = (l_1 + l_2)\frac{\partial}{\partial x_3} w_3,
\end{gathered} \tag{28}$$

and the uniaxial loading conditions

$$\bar{\sigma}_{22} = 0, \bar{\sigma}_{33} = 0. \tag{29}$$

The effective axial Young's modulus and Poisson's ratio are defined by

$$\bar{E}_A = \bar{\sigma}_{11}/\bar{\epsilon}_{11} \tag{30}$$

$$\bar{\nu}_A = -\bar{\epsilon}_{22}/\bar{\epsilon}_{11} \tag{31}$$

and they are determined from the solution of (28) and (29), in conjunction with (25)–(26).

When the composite is subjected to a uniaxial stress in the $x_2$-direction, such that $\bar{\sigma}_{22} \neq 0$, and all other $\bar{\sigma}_{ij}$ are zero, there are 26 nontrivial equations in the 26 unknowns $\phi_1^{(\alpha\beta\gamma)}$, $\chi_2^{(\alpha\beta\gamma)}$, $\psi_3^{(\alpha\beta\gamma)}$, $(\partial/\partial x_1)w_1$ and $(\partial/\partial x_3)w_3$, which are given by (28) and

$$\bar{\sigma}_{11} = 0, \bar{\sigma}_{33} = 0. \tag{32}$$

Here we define the effective transverse Young's modulus and Poisson's ratio of the composite in the form

$$\bar{E}_T = \bar{\sigma}_{22}/\bar{\epsilon}_{22} \tag{33}$$

$$\bar{\nu}_T = -\bar{\epsilon}_{33}/\bar{\epsilon}_{22} \tag{34}$$

which are computed from the solution of (28) and (32).

The effective plane strain bulk modulus, $\bar{k}$, which is not independent of the previous overall constants, can be determined directly from the solution of (28) by selecting $\bar{\epsilon}_{11} = 0$, $\bar{\epsilon}_{22} = \bar{\epsilon}_{33} = \epsilon_0$, yielding

$$\bar{k} = \bar{\sigma}_{22}/2\epsilon_0 = \bar{\sigma}_{33}/2\epsilon_0. \tag{35}$$

The effective axial shear modulus is determined by applying $\bar{\sigma}_{12} \neq 0$ (or $\bar{\sigma}_{13} \neq 0$), and all other $\bar{\sigma}_{ij} = 0$. It turns out that the resulting equations are sufficient for the determination of this modulus only in the limiting case of long fibers (for fibers of finite length the number of

unknowns exceeds by 2 the number of independent equations). The results of the self-consistent scheme method reported in[4, 5] however, indicate that the effective axial shear modulus is very weakly dependent on the aspect ratio.

## APPLICATIONS

In the following, numerous applications and assessments of the proposed theory are given and several comparisons with experiments and other approaches are presented and discussed.

(1) *Long-fiber composites*

As a first necessary check of the results provided by the present model, we consider long-fiber composites ($s \to \infty$; $h_1 = l_1$). In this limiting case, the model reduces to that presented previously in [6], for continuous fibers of square cross sections. It turns out that the resulting effective constants $\bar{E}_A$, $\bar{\nu}_A$, $\bar{k}$ and $\bar{G}_A$ where $\bar{G}_A$ is the effective axial shear modulus given by[6]

$$\bar{G}_A = \bar{\sigma}_{12}/(2\bar{\epsilon}_{12}) = \frac{\mu_2}{h_1 + h_2} \frac{\mu_1(h_1^2 + h_2^2 + h_1 h_2) + \mu_2 h_1 h_2}{\mu_1 h_2 + \mu_2 h_1} \tag{36}$$

with $\mu_1$, $\mu_2$ being the regidity of the fiber and matrix, respectively, are in *excellent agreement* with those provided by the composite cylinders model[7, 1]. The latter model effectively represents the long-fiber composite as a transversely isotropic material whose four constants $\bar{E}_A$, $\bar{\nu}_A$, $\bar{k}$ and $\bar{G}_A$ are given by closed form expressions. Extensive discussions of the effective moduli predicted by the composite cylinders model can be found in [1] and [7].

For the effective transverse Young's modulus $\bar{E}_T$, upper and lower bounds only can be obtained from the composite cylinders model, whereas in the present model it can be directly determined from (33). In Fig. 2(a), the transverse Young's modulus, $\bar{E}_T$, for a glass(1)/epoxy(2) long-fiber composite provided by the present model is compared with experimental data taken from[10]. The material constants are $E_1/E_2 = 21.19$, $\nu_1 = 0.22$ and $\nu_2 = 0.35$, where $E_1$, $E_2$ are the Young's moduli of the constituents and $\nu_1$, $\nu_2$ are their Poisson's ratios. It is well seen that the agreement between the theoretical and measured results is satisfactory.

Similarly, $\bar{E}_T$ is given in Fig. 2(b) for boron (1)/epoxy(2) long-fiber unidirectional composite where $E_1/E_2 = 100$, $\nu_1 = 0.2$ and $\nu_2 = 0.35$. Here too the agreement between the prediction of the present theory and the measured data (reported in[7]) is clearly noticed.

(2) *Bilaminated composites*

In the limit, when two sides of the rectangular parallelpiped (which represent the finite fiber) are very long with respect to the third, e.g. $h_1 \to \infty$, $l_1 \to \infty$ and $d_1$ is kept finite (see Fig. 1a), the case of a periodically bilaminated medium is obtained, in which $d_1$ and $d_2$ stand for the widths of the layers. The overall behavior of the laminated medium can be represented by a transversely isotropic material ($x_1$ is the axis of symmetry) whose effective constants have closed form expressions which were derived by Postma[8] and summarized in [1]. The values of the effective moduli, provided by the present theory in this limiting situation, are in excellent agreement (they apparently coincide) with those given by the exact expressions of Postma, thus indicating the reliability of the model in the present situation as well.

(3) *Particulate composites*

When the aspect ratio of the fibers is one ($s = 1$) the special case of a particulate composite is obtained, for which the filler concentration is given by eqn (24). For this value of $s$, the effective axial Young's modulus and Poisson's ratio, given by (30) and (31), coincide with the effective transverse Young's modulus and Poisson's ratio given by (33) and (34).

In Fig. 3(a) the effective Young's modulus and Poisson's ratio against $v_1$ are shown for a glass(1)/polyester(2) composite, for which the ratio of the Young's moduli of the constituents is $E_1/E_2 = 40.8$ and their Poisson's ratios are $\nu_1 = 0.21$, $\nu_2 = 0.45$. The theoretical curves are compared with the experimental results of Richard[11] and it is well seen that a good agreement exists.

When the particulate composite is described by the composite spheres model[9, 1], by which

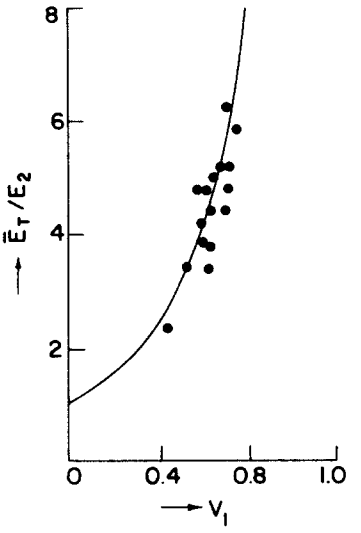


(a)

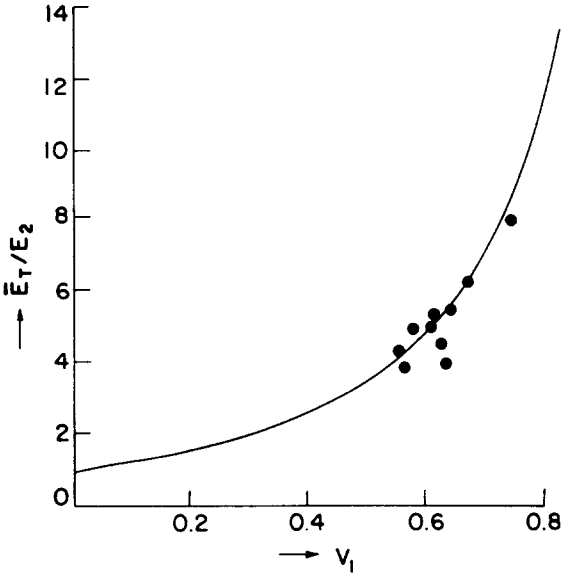


(b)

Fig. 2. (a) Comparison between the theoretical (——) and measured effective transverse Young's modulus for a long-fiber composite made of glass (1)/epoxy (2) for which $E_1/E_2 = 21.19$, $\nu_1 = 0.22$ and $\nu_2 = 0.35$. The experimental data are taken from[10]. (b) Same as (a), but for boron (1)/epoxy(2) unidirectional composite where $E_1/E_2 = 100$, $\nu_1 = 0.2$ and $\nu_2 = 0.35$. The experimental data are taken from[7].

the composite is represented by an equivalent isotropic material, it is known that only the resulting effective bulk modulus can be expressed in an exact form. It is given by

$$\bar{K} = K_2 + v_1(K_1 - K_2)/[1 + (1 - v_1)(K_1 - K_2)/(K_2 + \tfrac{4}{3}\mu_2)] \tag{37}$$

where the subscripts 1, 2 stand for the filler and matrix, respectively.

For the present model, the effective bulk modulus of the particulare medium can be determined directly from (28) by substituting $\bar{\epsilon}_{11} = \bar{\epsilon}_{22} = \bar{\epsilon}_{33} = \epsilon_0$ yielding:

$$\bar{K} = \bar{\sigma}_{11}/3\epsilon_0 = \bar{\sigma}_{22}/3\epsilon_0 = \bar{\sigma}_{33}/3\epsilon_0. \tag{38}$$

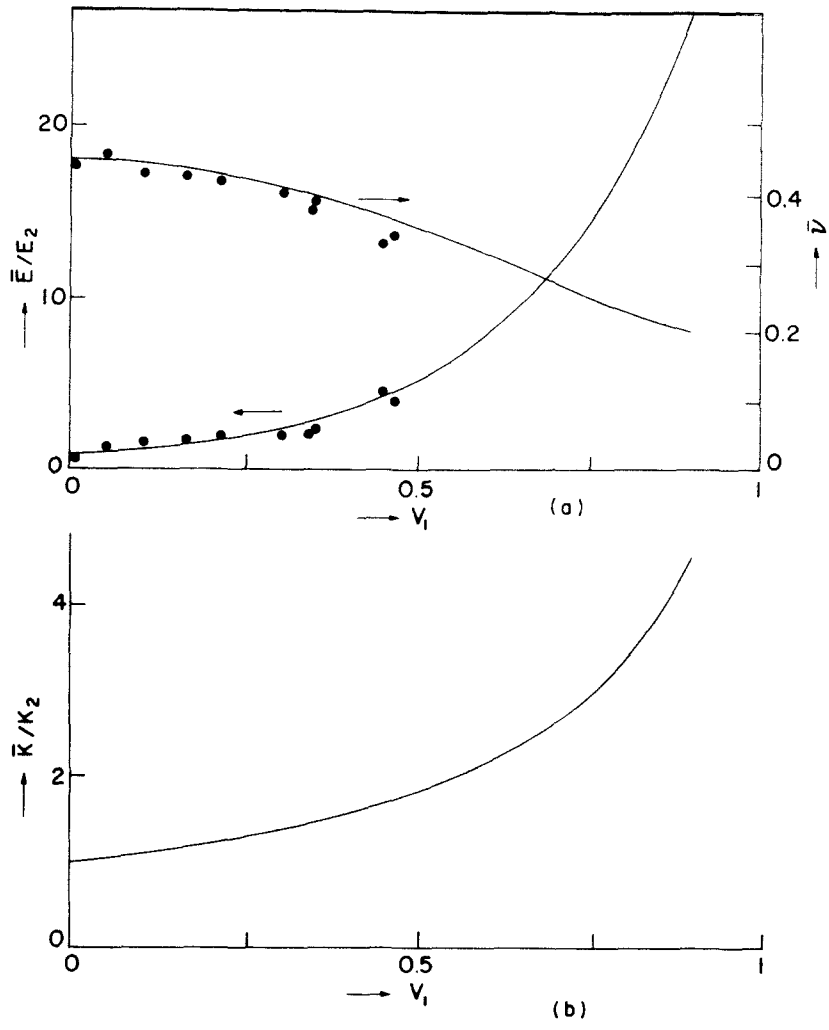


Fig. 3. (a) Comparison between the theoretical (——) and measured effective Young's modulus and Poisson's ratio for a particulate composite made of glass (1)/polyester (2) for which $E_1/E_2 = 40.8$, $\nu_1 = 0.21$ and $\nu_2 = 0.45$. The experimental data are taken from [11]. (b) A plot of the effective bulk modulus vs $v_1$ for the glass/polyester particulate composite. The corresponding curve based on (37) coincides.

In Fig. 3(b), the effective bulk modulus for the glass(1)/polyester(2) composite, computed from (38), vs $v_1$ is shown. It turns out that $\bar{K}$, given by the composite spheres model (37), is in excellent agreement with the prediction of the present model (38) (up to the scale of the plot they are indistinguishable).

It should be noted that the relation $\bar{K} = \bar{E}/(3-6\bar{\nu})$ is satisfied as can be expected.

As further checks for the veracity of predictions of the present theory for particulate composites, the effective Young's modulus is shown in Fig. 4(a) for sand(1)/epoxy(2) composite, for which $E_1/E_2 = 35.7$, $\nu_1 = 0.25$, $\nu_2 = 0.4$, together with the experimental results of Ref. [12], measured in compression and tension tests. The satisfactory agreement between the theoretical curve and experimental data is well observed.

In Fig. 4(b), theoretical and measured results for the effective Young's modulus of a porous epoxy matrix are shown, vs $v_1$ (which expresses in this case the amount of porosity). The present theory in this situation appears to predict higher values, especially for $v_1 > 50\%$. It is interesting to mention, however, that all the theoretical curves in Ref. [12, Fig. 3], based on various approaches, pass above the experimental data in this range. In [13], a model for a porous medium in the form of a periodic cubical structure of spherical voids (allowing a maximum porosity of $\pi/6 \approx 0.52$) was recently developed, and numerical results are given for $v_1 < 40\%$.

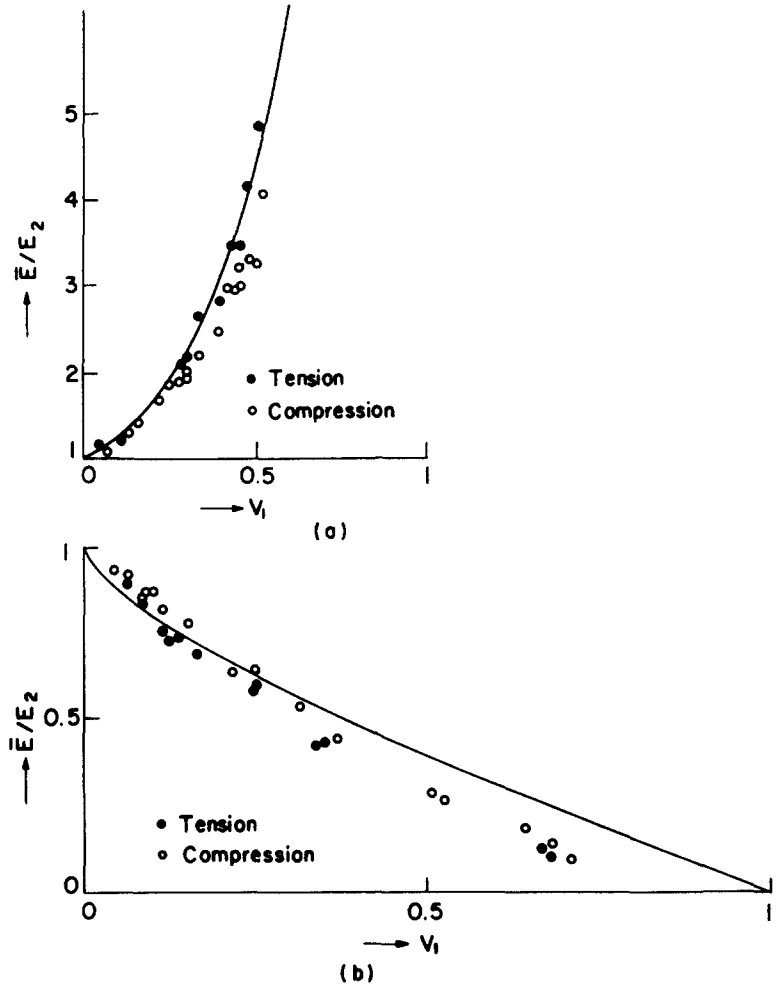


Fig. 4. (a) Comparison between the theoretical (——) and measured effective Young's modulus for a particulate composite made of sand (1)/epoxy (2) for which $E_1/E_2 = 35.7$, $\nu_1 = 0.25$ and $\nu_2 = 0.4$. The experimental data are taken from[12]. (b) Comparison between the theoretical (——) and measured effective Young's modulus of a porous epoxy vs the amount of porosity. The experimental data are taken from[12].

(4) *Short-fiber composites*

When the fibers aspect ratio is greater than one, a composite material with fibers of finite length, aligned in the $x_1$-direction, is obtained.

In Fig. 5(a), we present the graph of the effective axial Young's modulus, computed from eqn (30), vs the aspect ratio for a nylon(1)/rubber(2) composite for which the ratio of the Young's moduli of the constituents is $E_1/E_2 = 973$ and their Poisson's ratios are: $\nu_1 = 0.4$, $\nu_2 = 0.5$. The volume concentration of the nylon is $v_1 = 35\%$. In the same figure the experimental results of Kardos *et al.* [14] are included. It is clear that the comparison between the theoretical and measured values exhibits a good correspondence, which support the reliability of the theory. In[14], the experimental data are compared with the prediction of the Halpin–Tsai semi-empirical equation which turns out to coincide (in the given scale of the plot) with the theoretical curve of Fig. 5(a) for $s \geq 4$.

As another check of the validity of the present model, we show in Fig. 5(b) the measured values (taken from Ref.[14]) of the effective Young's modulus of the nylon/rubber composite when the short fibers are randomly oriented in the rubber matrix.

On the other hand, the theoretical values of the effective Young's modulus of planer and three-dimensionally random distribution of fibers can be determined, by using the method of Christensen and Waals[15, 1], directly from the effective moduli of the corresponding oriented short-fiber composite. The latter are given according to the present theory by (30), (31), (33),

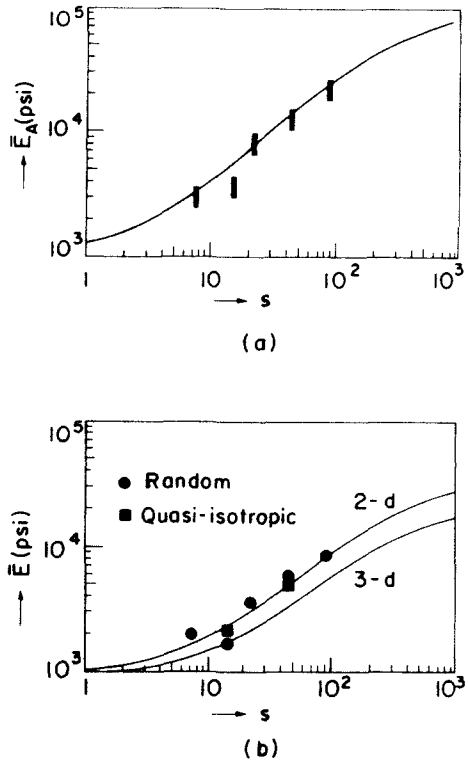


Fig. 5. (a) Comparison between the theoretical (——) and measured effective axial Young's modulus for an aligned-fiber composite made of nylon (1)/rubber (2) for which $E_1/E_2 = 973$, $\nu_1 = 0.4$, $\nu_2 = 0.5$ and $v_1 = 0.35$. The experimental data are taken from[14]. (b) Same as (a) but for randomly oriented fibers of planer (2-d) and three-dimensional (3-d) distributions.

(34) and (36). It should be noted that the expression for the effective axial shear modulus of oriented long-fiber composites (eqn 36) is used here since $\bar{G}_A$ is very weakly sensitive to the variation in the aspect ratio for a constant value of fibers concentration (see[4, 5]). The resulting computations of the effective Young's modulus are shown in Fig. 5(b) against the aspect ratio in the two cases of complete (3-dimensional) and planar (2-dimensional) random distribution of short fibers. It is seen that the experimental results fit very well with the theoretical curve of planer random distribution.

It is also possible to perform comparisons with the measured values, reported in[17], of the effective axial Young's modulus, $\bar{E}_A$, of steel (1)/epoxy (2) and copper (1)/epoxy (2) unidirectional short-fiber composites The material constants of the phases of the two composites are $E_1/E_2 = 76$, $\nu_1 = 0.3$, $\nu_2 = 0.35$ and $E_1/E_2 = 42$, $\nu_1 = 0.3$, $\nu_2 = 0.35$, respectively. The theoretical results (computed from eqn 30) and the experimental values are shown in Fig. 6. The curves shown in [17] which are based on semi-empirical equations are much higher than the measured values so that they are not useful.

The self-consistent scheme (s.c.s.) has been applied in [4] and [5] for the prediction of the effective behavior of aligned short-fiber composites. In the framework of this theory a single ellipsoidal inclusion of a given aspect ratio is assumed to be imbedded in a continuous homogeneous medium. The inclusion has the elastic properties of the short fiber, while the surrounding material has the effective properties of the composite. The solution of the single elastic inclusion problem is used for the determination of the effective constants of the composite. These assumptions give rise to some unrealistic descriptions of the composite, as it is discussed in [1].

In Fig. 7 we compare the results for the effective axial and transverse Young's modulus based on the present theory with the s.c.s. results of Chou *et al.*[5], for several values of the aspect ratio. The ratio of the Young's moduli of the composite's constituents is $E_1/E_2 = 20$, and their Poisson's ratios are $\nu_1 = 0.3$, $\nu_2 = 0.35$. It is seen that the curves based on the present model either partially coincide or are below the curves computed by the s.c.s. This feature

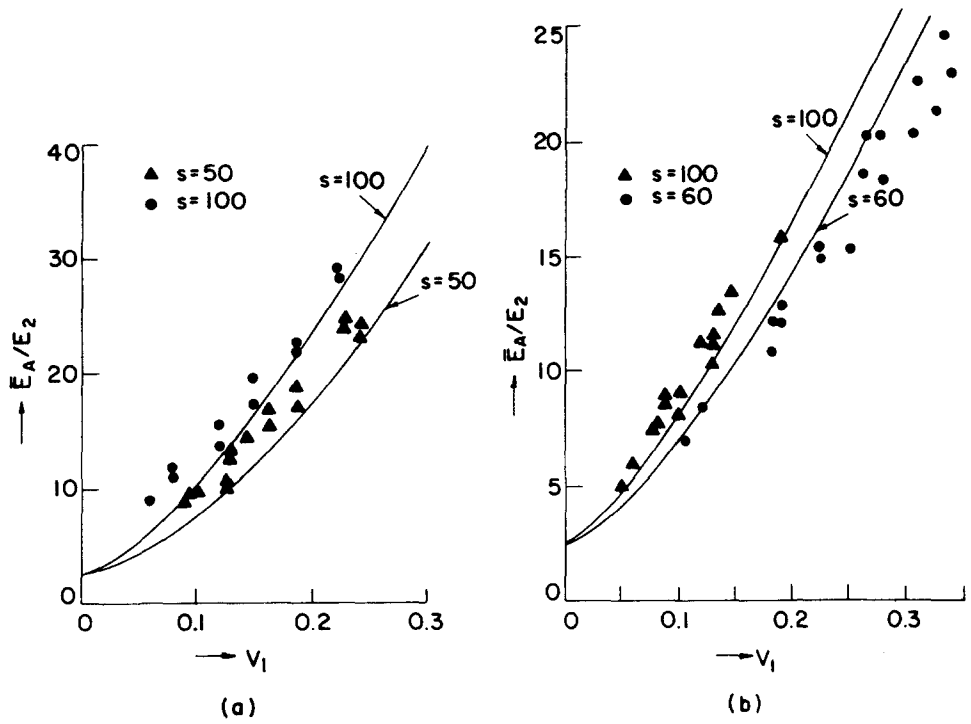


Fig. 6. (a) Comparison between the theoretical (———) and measured effective axial Young's modulus for two values of the aspect ratio, of an aligned short-fiber composite made of steel (1)/epoxy (2) for which $E_1/E_2 = 76$, $\nu_1 = 0.3$ and $\nu_2 = 0.35$. The experimental data are taken from[17]. (b) Same as (a) but for copper (1)/epoxy (2) composite for which $E_1/E_2 = 42$, $\nu_1 = 0.3$ and $\nu_2 = 0.35$.

appears to be consistent with the observation that the values of the effective Young's modulus of a particulate composite ($s = 1$) predicted by the s.c.s. are higher than the experimental data for $\nu_1 > 30\%$, see [11, Fig. 2], whereas the prediction of the present model is in a good agreement (see Fig. 3a). In addition, the relatively weak dependence of the effective transverse Young's modulus on the aspect ratio should be noted (this dependence is completely neglected in the Halpin–Tsai equations).

In addition to the theoretical s.c.s. results of Laws and McLaughlin[4], some experimental data for the effective axial Young's modulus of glass(1)/nylon(2) and glass(1)/polypropylene(2) short-fiber composites are reported. In Table 1 these experimental results, assuming perfect alignment of the fibers, are compared with the prediction of the present theory (eqn 30), as well as the results of the s.c.s. of[4]. Also included in the Table are the values given by the Halpin–Tsai equation[14] which is based on a semi-empirical approach. It is clearly observed that the experimental data are closer to the values predicted by the present theory, and the s.c.s. results are pronouncely above them.

Table 1. Results for the effective axial Young's modulus $\bar{E}_A$ of short-fiber composites

| composite | reinforcement ratio $v_1$ | aspect ratio s | $\bar{E}_A/E_2$ experiment | present theory | s.c.s. | Halpin-Tsai |
|---|---|---|---|---|---|---|
| glass(1)/nylon(2) $E_1/E_2 = 23$, $\nu_1 = 0.2$, $\nu_2 = 0.4$ | 17.7% | 18.6 | 3.1 | 2.8 | 4.34 | 3.63 |
| glass(1)/polypropylene(2) $E_1/E_2 = 47.36$, $\nu_1 = 0.2$, $\nu_2 = 0.4$ | 10.9% | 43.7 | 3.55 | 2.86 | 5.6 | 4.44 |

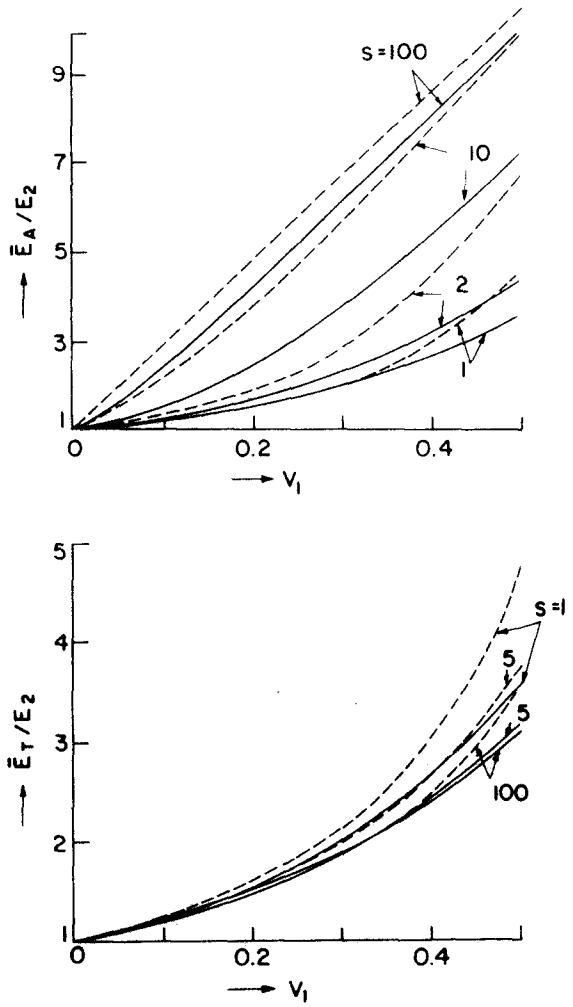


Fig. 7. Results of the effective axial and transverse Young's moduli provided by the present theory (——) and the self-consistent method of [5] (----) for several values of the fiber's aspect ratio with $E_1/E_2 = 20$, $\nu_1 = 0.3$ and $\nu_2 = 0.35$.

*Acknowledgement*—This research was sponsored by the Air Force Office of Scientific Research/AFSC under Grant AFOSR-80-0214, through the European Office of Aerospace Research and Development (EOARD), U.S. Air Force.

## REFERENCES

1. R. M. Christensen, *Mechanics of Composite Materials*. Wiley-Interscience, New York (1979).
2. W. B. Russel, On the effective moduli of composite materials: effect of fiber length and geometry at dilute concentrations. *Z. Angew. Math. Phys.* **24**, 581–600 (1973).
3. N. Phan-Thien, A micromechanic theory of chopped-fiber-reinforced materials. *Fiber Sci. Tech.* **13**, 423–433 (1980).
4. N. Laws and R. McLaughlin, The effect of fiber length on the overall moduli of composite materials. *J. Mech. Phys. Solids* **27**, 1–13 (1979).
5. T. W. Chou, S. Nomura and M. Taya, A self-consistent approach to the elastic stiffness of short-fiber composites. *J. Composite Matls* **14**, 178–188 (1980).
6. J. Aboudi, A continuum theory for fiber-reinforced elastic-viscoplastic composites. *Int. J. Engng Sci.* **20**, 605–621 (1982).
7. Z. Hashin, Theory of fiber reinforced materials. *NASA Rep. Contract NASA* 1-8818 (1970).
8. G. W. Postma, Wave propagation in a stratified medium. *Geophysics* **20**, 780–806 (1955).
9. Z. Hashin, The elastic moduli of heterogeneous materials. *J. Appl. Mech.* **29**, 143–150 (1962).
10. S. W. Tsai and H. T. Hahn, *Introduction to Composite Materials*. Technomic, Westport (1980).
11. T. G. Richard, The mechanical behavior of a solid microsphere filled composite. *J. Composite Matls* **9**, 108–113 (1975).
12. O. Ishai and L. J. Cohen, Elastic properties of filled and porous epoxy composites. *Int. J. Mech. Sci.* **9**, 539–546 (1967)
13. S. Nemat-Nasser and M. Taya, On effective moduli of an elastic body containing periodically distributed voids. *Q. Appl. Math.* **39**, 43–59 (1981).
14. J. L. Kardos, J. C. Halpin and L. Nicolais, Mechanical Properties of Semicrystalline Polymers Regarded as Composite

Materials. In *Theoretical Rheology* (Edited by J. F. Hutton, J. R. A. Pearson and K. Walters), pp. 186–205. Applied Science, London (1975).
15. R. M. Christensen and F. M. Waals, Effective stiffness of randomly oriented fiber composites. *J. Composite Matls* **6**, 518–532 (1972).
16. J. C. Halpin and N. J. Pagano, The laminate approximation for randomly oriented fibrous composites. *J. Composite Matls* **3**, 720–724 (1969).
17. J. M. Berthelot, Effect of fibre misalignment on the Elastic properties of oriented discontinuous fibre composites. *Fiber Sci. Tech.* **17**, 25–39 (1982).